Available online at www.sciencedirect.com
SCIENCE DIRECT®
European Journal of Pharmaceutics and Biopharmaceutics 58 (2004) 369–383
European Journal of Pharmaceutics and Biopharmaceutics
www.elsevier.com/locate/ejpb

Review article

The use of asymmetrical flow field-flow fractionation in pharmaceutics and biopharmaceutics

Wolfgang Fraunhofer[a,*], Gerhard Winter[b]

[a]Abbott GmbH and Co. KG, Department Pharmaceutical Development, Ludwigshafen, Germany
[b]Department of Pharmacy, Pharmaceutical Technology and Biopharmaceutics, Ludwig-Maximilians-University, Center for Drug Research, Munich, Germany

Received 12 January 2004; accepted in revised form 8 March 2004

Available online 1 June 2004

Abstract

Field-flow fractionation (FFF) is a family of flexible analytical fractionating techniques which have the advantage that the separation of analytes is achieved, solely through the interaction of the sample with an external, perpendicular physical field, rather than by the interaction with a stationary phase. The rapid progress in pharmaceutical biotechnology goes along with an increasing demand in potent, high-efficient analytical methods. Thus, FFF techniques are gaining increasing attention for their ability to separate and characterize populations of polymers, colloids and particles of up to about 100 μm in size. It is the intention of this review to provide an overview on common FFF techniques, to summarize inherent advantages and limitations and to introduce both established and challenging applications in the (bio)pharmaceutical field. Thereby, asymmetrical flow FFF is addressed predominantly, since it is the most versatile applicable FFF technique.

Keywords: Field-flow fractionation; Separation; Biopharmaceutical application; Protein analytics; Particle characterization; Review

1. Introduction and underlying principles

FFF-conceptualized in the late 1960s [1]—occupies a unique niche in the field of analytical fractionations because it is virtually the only technique being capable of separating materials from lowest nm-range over the entire colloidal size range up to two-digit μm-range with high resolution [2]. Thereby, one obstacle to a widespread FFF utilization is due to its greatest asset, its versatility, and this versatility comes along with a price: there is no simple formula for choosing the proper FFF technique and the optimal separation parameters for a given application. One has to understand the underlying mechanisms to perform a separation problem by means of FFF. Although, optimal conditions provided, applications and separation tasks prevalently considered impractical or at least highly challenging can be successfully approached.

The FFF sample separation is performed inside a narrow ribbon-like channel. This channel typically reveals dimensions of ±50 cm in length and ±2 cm in width, whereas the channel height can vary between 50 and 500 μm. From the inlet, a carrier liquid is pumped through the channel, establishing a parabolic laminar Newtonian flow profile as in a capillary tube, propelling the samples towards the outlet [3,4]. Perpendicular to the direction of the carrier liquid flow an external field is applied, forcing the sample components to accumulate at one of the channel walls, termed accumulation wall. Under normal mode conditions the sample components can be considered as non-interacting point masses, with their center of gravity near to the accumulation wall. Due to the established concentration gradient, a diffusion flux in reverse direction, i.e. back into the interior of the channel, is induced according to Fick's law. As a consequence of the two rival parameters—the exerted field of force and the opponent diffusion flux—a steady-state profile is generated, and the equilibrium distributions of the sample components across the channel can be expressed by a mean layer thickness [5,6]. Those analytes with distributions nearest to the accumulation wall (like X) are positioned in slower flow laminae of the parabolic laminar flow. Accordingly, they gradually separate from analytes which are positioned

* Corresponding author. Abbott GmbH and Co. KG, Department of Pharmaceutical Development, Knollstr., 67008 Ludwigshafen, Germany. Tel.: +49-621-589-1210; fax: +49-621-589-1212.
E-mail address: wolfgang.fraunhofer@abbott.com (W. Fraunhofer).

0939-6411/$ - see front matter © 2004 Elsevier B.V. All rights reserved.
doi:10.1016/j.ejpb.2004.03.034

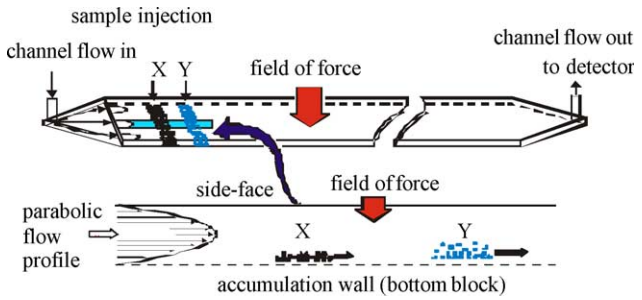

Fig. 1. Schematic representation of the FFF separation of two components X and Y across the parabolic flow profile within the channel. Due to its higher diffusion coefficients D, smaller analytes (fraction Y) are positioned at elevated channel heights in faster flow laminae, thus eluting prior to larger analytes (fraction X). Samples with small D values cannot efficaciously oppose the force field exerted and accumulate near the bottom wall in slower flow laminae.

at more elevated levels in the channel (like Y), therefore eluting with faster laminae (Fig. 1).

Consequently, FFF can be considered as a hybrid of chromatography and field-driven methods such as electrophoresis and ultracentrifugation [7,8]. Like chromatography, FFF is an elution technique with inherent differential flow displacement phenomena. On the other hand, like ultracentrifugation, FFF separation is based on an applied gradient or field of force.

Since that field of force is opposed by sample diffusion processes, the sample concentration c (relative to the wall concentration c_0) approaches an exponential function of the mean layer thickness x remote from the accumulation wall [9]:

$$c = c_0 \exp\left(\frac{-x|U|}{D}\right) \tag{1}$$

where U represents the drift velocity of the sample induced by the external field. The diffusion coefficient D can be related to the frictional coefficient f by means of the Stokes–Einstein relationship

$$D = \frac{kT}{f} \tag{2}$$

with k as Boltzmann's constant and T as the temperature. The drift velocity U is correlated to the force F, which is exerted on the sample, by $U = F/f$. The mean sample-wall distance l, derived by $l = D/|U|$, leads to

$$l = \frac{kT}{F} \tag{3}$$

expressing that the samples will be positioned proximate to the accumulation wall (low l) when exposed to vigorous forces. In order to provide optimal values of l, i.e. to guarantee appropriate sample levels for FFF experiments, the intensity of the external field can be varied. Accordingly, F can be altered proportionally and the precedent condition to ensure efficient FFF operations can be met: channel height $w \gg l$. As the FFF accessories kits available provide almost any w, the wide application range of FFF becomes evident. Eq. (3) can be extended by the dimensionless parameter λ, leading to

$$\lambda = \frac{t_0}{t_r} = \frac{V_0}{V_r} = \frac{l}{w} = \frac{kT}{Fw} \tag{4}$$

where λ is a synonym for the retention ratio R, i.e. the retention time of an unretained sample component t_0 to the retention time of a retained sample component t_r, or equivalently in terms of retention volumes V_0/V_r. It is important to refer to the relationship $t_r \sim F$ given by Eq. (4), thereby implying that the retention time of sample components can be assessed as desired by exerting expedient force intensities. Besides for sample fractionation, FFF can advantageously be installed for assessing physical sample parameters: given the known parameters t_0, V_c, V_0 and w, furthermore the experimentally assessed t_r, and assuming the approximation $R = 6\lambda$, the diffusion coefficient D can be obtained directly via

$$D = \frac{t_0 V_c w^2}{6 t_r V_0} \tag{5}$$

Moreover, by applying the Stokes–Einstein relationship—referred to in Eq. (2)—the hydrodynamic diameter d_H of sample specimen can be assessed.

$$d_H = \frac{2kTV_0}{\pi\eta V_c w^2 t_0} t_r \tag{6}$$

where η is the solvent viscosity. Therefore, FFF not only enables the fractionation of sample components, but also can be utilized for concomitant size determination of the fractionated specimen [5]. However, the assessment of sample dimensions by means of FFF theory per se has taken a back seat in recent years, for several reasons. The reliability of the t_r values determined has to be scrutinized, e.g. due to sample-membrane interactions potentially biasing FFF data. More importantly, other sophisticated size-assessing detection systems are to be preferred, primarily multi-angle light scattering (MALS) [10]. The pioneering experiment was performed not until 1991, when MALS was combined with sedimentation-FFF [11]. The first successful coupling of MALS with flow-FFF was performed shortly afterwards, in order to determine molar mass distributions of polystyrene particles and dissolved dextranes [12]. Recently, FFF was coupled with time-of-flight mass spectrometry [13,14].

Large analytes with low diffusion coefficient, D, values will offer only slight resistance to exerted force intensities. In contrast, smaller analytes such as peptides or low molecular weight (lmw) proteins will counterbalance even extensive force fields, due to their high D values. This explains why it is usually more delicate to separate small sample specimen via FFF than to fractionate larger samples. As it will be shown later on, F can be increased to a level at which the elution of high molecular weight (hmw) samples is heavily delayed. By monitoring of the channel effluent by

adequate detection systems, the retention times of the analytes can be determined and sample compositions can be elucidated by straightforward FFF experiments.

The magnitude of F, which can be applied on the sample specimen, depends on the experimental arrangements of the various FFF techniques, i.e. the kind of field that is installed. Primarily four prominent FFF fields have become most relevant for scientific research—and are applied to an increasing extent in industrial practice [15]. The common feature of all FFF subtechniques is the parabolic flow profile of the carrier liquid as the driving parameter of separation.

2. Various FFF techniques

2.1. Sedimentation FFF (SdFFF)

Since the theoretical principles of SdFFF were introduced in the late 1960s and put into practice shortly thereafter, SdFFF may be deemed one of the oldest FFF techniques [16,17]. SdFFF experiments are performed in a channel constituted by two closely spaced parallel surfaces. When this channel is rotated in a centrifuge, dissolved and suspended analytes—which are more dense than the ambient mobile phase—are forced to migrate towards the outer wall. Correspondingly, if the sample is less dense than the ambient liquid, floating phenomena can be observed, and those sample components accumulate at the inner wall. The limiting particle size for retention in SdFFF depends on the maximum speed of the centrifuge, i.e. on the gravitational field exerted. Via modern SdFFF equipment with inherent gravitational forces exceeding 100,000 g, a broad range of materials can be characterized, with typical application ranges of >25 nm (particles) and $>10^6$ g/mol (polymers). The aqueous carrier density can be varied towards lower densities by adding organic liquids. Vice versa, the density will increase if salts or sugars are added to aqueous liquids or if water is added to organic fluids, respectively [18,19]. The theoretical principles of SdFFF are summarized by Eq. (7)

$$F = \frac{\pi d_H^3 G|\Delta\rho|}{6} \tag{7}$$

with G symbolizing the centrifugal/gravitational acceleration, $|\Delta p|$ the density differences between the sample components and the solvent used, and d_H the effective spherical diameter of the sample component. Due to the high resolution potential of SdFFF, typical applications are the separation of biopolymers and macromolecules [20], cell sorting [21,22] or the characterization of sediment colloids [23,24].

2.2. Thermal FFF (ThFFF)

ThFFF is considered the oldest of all FFF methods. Research in thermal diffusion started in 1856, when Ludwig observed the selective migration of compounds towards colder regions [25]. In the 1960s, ThFFF was at first applied for the separation of polystyrenes [26,27], and its broad applicability for the fractionation of various polymers was demonstrated in 1978 [28]. The channel design of ThFFF is shown in Fig. 2.

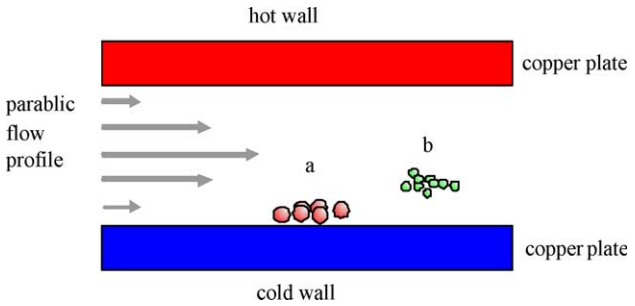

Fig. 2. Basic illustration of a ThFFF channel. Note that the sample components, e.g. lipophilic polymers, accumulate at the cold channel wall.

By exerting a large temperature difference across the channel the thermal diffusion effect is employed to concentrate the sample components—typically polymers and colloids—at the cold wall. Under normal operation, this temperature difference between the hot wall, heated with electric cartridges, and the water-cooled cold wall encompasses 100 °C. The applicability of ThFFF in aqueous systems is restricted due to the weak thermal diffusion of polymers in water. Therefore, lipophilic polymers $>10^4$ g/mol and particles are favorably characterized in organic media [29]. Given the background of the numerous assumptions inherent to ThFFF, this method is judged to be the most complicated FFF subtechnique. The effective driving force $|F|$ per analyte can be defined by

$$|F| = kT\frac{D_T}{D}\frac{dT}{dx} \tag{8}$$

with D_T as the thermal diffusion coefficient [5]. Although considerable effort is invested in the subject, e.g. by the development of micro-channels with increased speed and resolution power [30], ThFFF most likely will not gain acceptance in pharmaceutical analytics because of its inherent drawbacks due to the underlying principles. However, ThFFF occupies a niche in the spectrum of hmw polymer characterization, attributed to its unique separation mode [31–33].

2.3. Electrical FFF (elFFF)

In terms of its analytical properties, elFFF is discussed controversially. The prevalent elFFF channel design utilizes two graphite plates which serve a dual role of both channel wall and electrode, separated by a Teflon spacer [34]. Exposing the ~150 μm high channel to only a few volts gives rise to substantial effective field strengths in the order of 100–200 V m^{-1}. To achieve fields of comparable strength in capillary electrophoresis, 20–30 kV are to be

provided. Generally, electrophoretic separations lack the possibility of differentiating between particulate analytes of different size, but with similar surface charge density [35].

Since the electrical field E is related to the drift velocity U of a sample component with the electrophoretic mobility μ_e by $U = \mu_e E$, the force F exerted on the sample can simply be expressed by $D = \lambda \mu_e E w$. What speaks in favor of the method is the simplicity of applying and programming E, as does the absence of any moving parts. The other side of the elFFF medal is labeled with two major disadvantages: the electrode polarization limits the aqueous carrier solutions which can be applied and, as a consequence, the sample materials that can be characterized [36]. Additionally, conductivity differences between the analytes and the carrier liquid influence the retention, what means that sample concentration affects the data obtained [37,38]. A trend is evident, that more effort will be put into further development of other existing FFF subtechniques.

2.4. Flow FFF (F4)

The significant difference between F4 and the FFF subtechniques introduced above is that the separation field of force is established by a second stream of carrier liquid, pumped in vertical direction to the axial flow stream, as illustrated in Fig. 3. The F4 experiments are performed in a symmetrical set-up, in which the channel walls consist of two porous frits. This symmetrical system was developed in the mid 1970s [39]. The lower wall is covered by an ultrafiltration membrane, permeable only to carrier liquid, not to sample components. Provided by a separate pump, the cross-flow volume enters the channel via the upper channel wall, crosses the channel interior and finally passes the accumulation wall, subsequent to passing an ultrafiltration membrane. As the separation only relies on differences in diffusion coefficients, F4 is the most applicable FFF subtechnique, demonstrated in aqueous and organic mode characterizations of analytes ranging from solutes with inherent molar masses of ~500 g/mol and dimensions of <2 nm up to particles with dimensions of 100 μm [40]. The lower size limit is determined by the molecular weight cut-off of the ultrafiltration membranes (~1 kDa), whereas the upper size limit is assessed by a threshold of about 20% of the channel height [41].

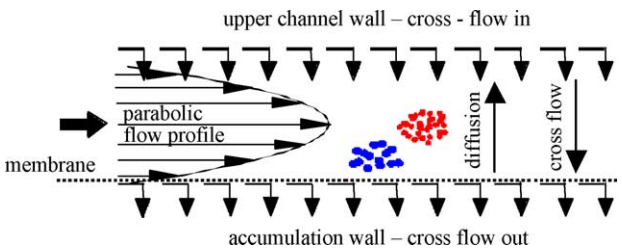

Fig. 3. Schematic representation of a Flow-FFF channel. The position of sample specimen is determined by two independent flow streams, i.e. the axial carrier liquid flow and the vertical cross-flow, propelling the sample components towards the accumulation wall.

The driving force of F4 separations, exerted on the analytes by the cross-flow, acts on all sample compounds with identical intensity and the separation of sample components is only due to differences in their inherent dimensions, i.e their diffusion coefficients D.

Still in the 1970s, a broad variety of samples was exemplarily separated by means of F4, covering polystyrene latexes, various proteins, viruses and macromolecules [42–45]. In retrospect, the further development of F4 seems predicted, confirming the golden rule of science: new techniques attract more successful experiments, successful experiments attract more users, more users contribute new ideas. In case of F4, Granger, Wahlund and Giddings helped to get a new idea accepted: the idea of an asymmetrical F4 channel set-up [46,47]. Besides the FFF subtechniques already addressed, a variety of other subtechniques exists. The majority of those attract scant attention and are only sporadically described in the literature, e.g. acoustic or photophoretic FFF. For extensive insight into FFF techniques and principles the reader is referred to comprehensive reviews [5] and handbooks [48].

2.5. Asymmetrical flow FFF (AF4)

AF4 draws a significant distinction to F4 in the channel set-up, revealing only one permeable wall, so that carrier liquid can leave the channel solely via the accumulation wall to generate a cross-flow. The upper wall normally consists of transparent plexiglas (polymethylmethacrylate, PMMA), non-permeable to the solvent (Fig. 4). The transparency of the upper wall allows visual observation of the channel interior, helping to cope with trouble-shooting during experiments or enabling visual monitoring of colored sample separation. Due to the obvious differences between upper and bottom wall, 'asymmetrical' was prefixed to the term Flow-FFF. Consequently, the cross-flow rate through the accumulation wall—comprising a ceramic frit covered by an ultrafiltration membrane—is induced by the constant loss of axial flow occurring with the transport of carrier liquid along the channel. This leads to a continuous decrease in the volumetric flow rate, i.e. the flow velocity of the axial flow, while approaching the outlet of

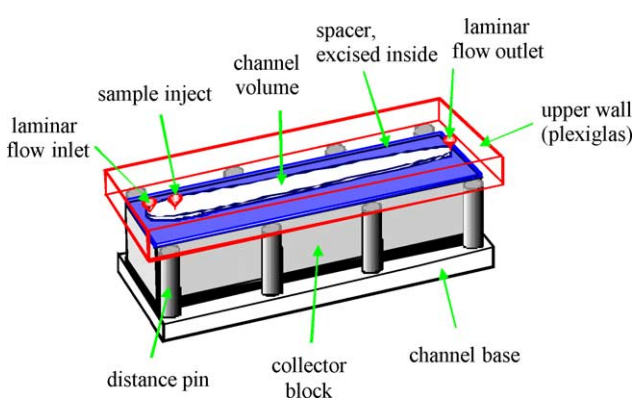

Fig. 4. Schematic presentation of the AF4 channel assembly.

the rectangular channel [49]. In case of using very thin channels with low volumetric capacities in order to speed up separations, applying high cross-flow rates results in fatal low outlet flow rates. During separation, this phenomenon has to be taken into account in order to avoid misassigning of sample characteristics due to the observed elution times. To compensate for these undesired effect, a trapezoidal channel geometry was innovated, where the with decreases ongoing towards the channel outlet. Within a short time, the trapezoidal channel proved superior to the traditional rectangular geometry, and represents the favored system today [5,50].

The suitability of a broad variety of wall materials such as polycarbonate, polyethylene, aluminium or stainless steel have been examined [51]. The introduction of modern materials such as PMMA not only broadened AF4 applicability, but also initiated the development of innovative channel construction: traditionally, spacers were sandwiched between both walls, dimensioning a definite channel height due to their gauge. Channel shape, e.g. rectangular or trapezoidal, was assessed by an outline cut in the spacer material, for instance polyester like mylar, teflon or polyimide [52]. Contrarily, a new way of channel construction is as simple as effective: via engraving an appropriate cavity—with desired depth and geometry—direct into the upper wall, the required channel volume capacity is provided. The wall block, with the cavity underside, is then placed on the ultrafiltration membrane, which overlies the ceramic frit.

The minimum useable channel height, i.e. the cavity depth, is determined by the compressibility of the ultrafiltration membrane [53,54]. When the channel is bolted together, the membrane is compressed in regions directly contacting the spacer and the upper wall, respectively. On the other hand, in unaffected areas the membrane maintains its original thickness and now protrudes into the channel. Amplified by membrane swelling phenomena, this determines a threshold for spacer thickness minima [41]. That is an important factor, as thin channels normally reduce separation time. Applying thin channels can be associated with the drawback of increased probability of interferences with the laminar forward flow profile. This, as a consequence of membrane corrugations, can detract from data verability, since the process of separation happens in immediate vicinity of the membrane. Considering that in normal mode separations the sample specimen are positioned in lamina levels not exceeding 5 μm distance off the membrane, the importance of smooth, unruffled membrane surfaces becomes evident.

During separation, the sample components are subjected both to an axial flow vector—as a result of the laminar forward flow—and to a transversal flow vector, arising from the cross-flow [55]. If the sum of the vector net effect is falsified by sterical barriers, reproducibility, accuracy, and power of the fractionation process can be critically corrupted. This, in combination with the imperative of sample-membrane compatibility, led to a rushing demand for various membrane materials. Cellullose derivatives, poly(ether)sulfone, polycarbonate, polyamide, acrylic copolymers, fluoropolymers, polyethylene and polypropylene are popularly used. Meanwhile, the prevalently used ultrafiltration membranes have to withstand fierce competition by microporous membranes, since the latter provide a flat surface, marginal compressibility, high flux and low cost.

As the samples are prevented from leaving the channel with the cross-flow by the membrane, its cut-off properties crucially influence potential sample loss and sample recovery. The nominal cut-off value only refers to an estimation of the smallest analyte retained by the membrane, far apart from a precise specification. Consequences arising therefrom can be for good or for bad: sample specimen with molar masses as low as 6.5 kDa have been observed to be retained by membranes with declared nominal pore sizes of 50 nm [56]. Otherwise, membrane permeability may provide optimal conditions in the analysis of lipoproteins and pharmaceutical colloids, where coanalytes like lmw plasma proteins present with the would interfere analytics, but are displaced from the samples by passing the membrane [57].

The (mathematical) considerations outlined above apply exclusively for what is often referred to as the normal or Brownian mode of FFF: sample specimen behave as point masses whose sizes are insignificant compared to the dimensions of the sample specimen zone. Consequently, sample retention becomes a unique reflection of the size, i.e. the hydrodynamic radius, and the diffusion coefficient [58].

The larger the sample specimen, the less valid this approach becomes. In case particle sizes increase to a level where they are no longer negligible compared to the channel height, their retention has to be considered as a reflection of their inability to approach infinitely close to the accumulation wall [59]. Because the centers of gravity of large particles can approximate the wall not closer than the particle radius, the net result of this protrusion into the parabolic flow profile is that migration becomes forwarded in relation to particle size (Fig. 5).

Thus, the order of separation is reversed, and that phenomenon is called steric mode effect [60]. The transition

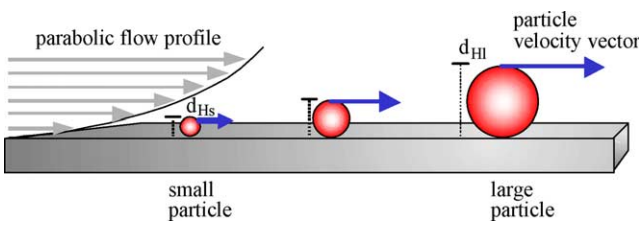

Fig. 5. Schematic representation of the steric mode FFF principle. Sample specimen are prevented from approaching the accumulation wall closer than half of their hydrodynamic diameter d_H. Due to their greater migration velocity vector, larger particles (d_{HI}) elute prior to smaller samples (d_{Hs}), vice versa to the normal mode situation.

between normal and steric FFF mode depends on both particle size and channel height and is to be assessed for standard separation parameters at ~1 μm. Though, there is more to that: it has been discovered early that steric particles do not migrate with direct contact to the wall surface—due to their high sensitivity to driving forces of the vertical field of force—but are positioned at elevated levels due to the role of hydrodynamic lift forces [61]. These results were substantiated by data revealing that large diameter particles are migrating at levels more distant from the accumulation wall than smaller particles, eluting also in steric mode [62]. The situation when steric mode is combined with hydrodynamic lift forces is generally referred to as hyperlayer mode.

Steric exclusion observed in areas adjacent to walls is an important parameter in other separation contexts, too, e.g. hydrodynamic chromatography or in size exclusion chromatography, where it accounts for the Casassa model [63,64].

Basically, the AF4 experiment can be divided into three stages: sample injection, sample focusing, and the fractionation step. Identical to conditions in HPLC, the sample volume designated to AF4 analysis is gauged by using sample loops with loop volumes spanning 10–100 μl. Considering prevalent AF4 channel capacities ranging between 200 and 1000 μl, the injection of 100 μl sample entails a considerable part of the channel volume being replenished by the sample, not to mention void volumina of the injection capillaries. In a worst case scenario, the injected sample would fill the channel completely. Starting fractionation subsequently would implicate a situation, in which some of the sample components were positioned directly adjacent to the flow inlet and the sample injection port, while the rest of the sample would populate areas towards the flow outlet. Fractionations based on those preliminary conditions would suffer insufficiency and peak broadening.

Hence, sample specimen are to be positioned in steady-state equilibrium levels before being eluted, in order to optimize fractionation quality. A focusing step—often termed focusing/relaxation step—must be performed prior to separation. Due to this, sample material distributed widely throughout the channel interior is forced into a narrow 'band' from which proper separation is possible [65]. Unlike other forms of FFF, the field of force in AF4 cannot be controlled independently of the axial flow. Therefore, sample focusing to narrow bands—to minimize band broadening of the detection signals—and sample arrangement in steady-state equilibrium profile has to be achieved simultaneously.

To meet this premise, an opposing stream of carrier liquid is pumped into the channel from the outlet end additionally to the carrier flow through the inlet port. As a consequence, the sample specimen are focused at a predetermined point in the vicinity of the sample injection port and the carrier liquid exits the channel via passing the membrane (Fig. 6). A position ~5 mm downstream of the inlet port is deemed an adequate location for sample focusing, since otherwise one has to accept the consequences of flow inhomogeneities: surface protuberances of both flow inlet port and sample inlet port may interfere with the axial parabolic flow profile and may foster artifacts [49].

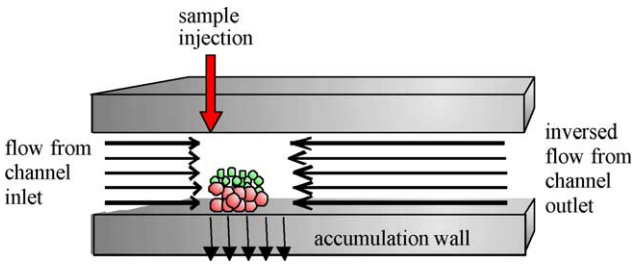

Fig. 6. Schematic diagram of sample specimen arrangement at the end of the focusing/relaxation step. Note that analytes are focused to a narrow band and arrange at level heights related to their diffusion coefficients.

Referring to Fig. 6, the dependence of successful AF4 separation on optimal focusing/relaxation becomes evident. Although the assessment of necessary focusing/relaxation times was approached mathematically, this calculation is considered to inhere some uncertainties due to the necessity of assumptions [66]. In AF4 practice, for quality monitoring of focusing/relaxation the utilization of color indicator substances like bromophenol blue is feasible.

In contrast to separation methods with rather stringent separation modes like SEC, the cross-flow intensity in AF4 can be changed and programmed arbitrarily during separation. This programming consists of intentionally and systematically varying the cross-flow rate—and commensurate herewith, the axial forward flow rate also has to be adapted. Already in the first paper, the concept of programming FFF runs was proposed and implemented shortly afterwards [1,27].

The delivery of facts in terms of programming by FFF practitioners was increasingly accompanied by theoretical concepts of theoreticians. A wide mathematical arsenal evolved in the FFF realm, including step, linear, parabolic and exponential functions, a special class of power functions capable of yielding almost constant relative resolutions, and data analysis algorithms [67–69]. By varying the cross-flow strength between individual runs by run programming, the correlation between cross-flow intensity and resolution power can be demonstrated (Fig. 7). With no cross-flow applied, the human serum albumin (HSA) specimen are eluting concomitantly, unifying in one peak in subsequent UV_{280} detection. The higher the cross-flow, the more efficient the separation, and at apt conditions HSA can be separated into monomer, dimer, trimer, and higher oligomer fractions.

The easiest way to describe the actual cross-flow intensity is simply to quote %—values. For example, 10% cross-flow with 1 ml/min detector flow condition means that elution medium enters the channel with a 1.11 ml/min flow volume. While passing the channel, 10% of the elution

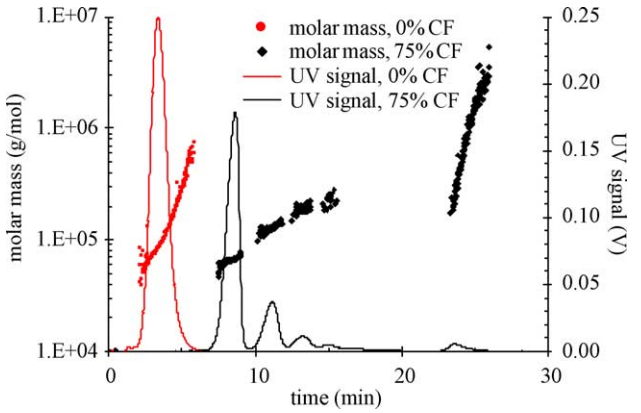

Fig. 7. Fractionation of HSA applying 0 and 75% cross-flow intensities. Minimizing the 75% cross-flow to 0% after 20 min enables elution of hmw aggregates, revealing molar masses of $>10^6$ Da. Detection with multi-angle light scattering (MALS) enables convenient UV data interpretation, assigning calculated masses to the peaks of monomer (66.9 kDa), dimer (133.8 kDa) and trimer (204 kDa), matching the theoretical values. Note that the UV signal of 0% cross-flow analysis unifies all HSA specimen, running the gamut from monomer to hmw aggregates.

medium are pumped off through the ultrafiltration membrane to generate a cross-flow profile of ~0.11 ml/min. The resulting laminar flow profile at the channel outlet remains unchanged at 1.0 ml/min. This is the more important, since basically all state-of-the-art detection systems applied in monitoring the elution of fractionated analytes—i.e. spectrophotometry, refractive index, light scattering and fluorescence detection units—are prone to artifact measurements due to (rapid) change of system parameters, i.e. discharge shifts of cell flow.

3. Selected applications of AF4/F4

Products of modern pharmaceutical biotechnology represent a very significant fraction of today's total pharmaceutical market. Thus far, some 90 recombinant proteins/monoclonal antibody-based products have gained marketing approval within the European Union, accounting for a 36% share of all new EU drug approvals since 1995 [70]. Bearing in mind the still unbroken boom in pharmaceutical biotechnology—the world market in recombinant drugs totalled US$ 27 billion in 2001 and is forecasted to almost double to US$ 50 billion in 2010—coping with challenging analytics, e.g. tasks like separation and characterization a broad variety of analytes present in one sample, will gain increasing importance in biotechnology.

3.1. Biopolymers—soluble analytes

In the majority of cases, biopolymeric applications of AF4/F4 refer to protein analysis. Subsequent to the first protein separation in 1977 [43], numerous proteins were investigated, including bovine and human serum albumin, γ-globulin, thyroglobulin [2,71–73], aldolase and ferritin [74,75].

Yet, in the course of reviewing AF4/F4 biopolymeric applications, it is to be accentuated that AF4 nowadays is not to be considered a well-known state-of-the-art method, neither in industries nor in scientific research. A general survey of the published literature in terms of AF4/F4 in protein analytics is completed within short time, revealing a low two-digit number of extensive scientific publications. In contrast, to perform the same in terms of HPLC means to become assailed with thousands of articles. This indicates that AF4 applications hitherto mainly originated for special analytical tasks. However, being bolstered with considerable advantages and having experienced further developments in the last decade, AF4/F4 utilizations in protein analytics are surging.

The acid test for any separation technique is providing greatest resolution within shortest time, thereby avoiding the generation of artifacts. Since AF4 is equipped with field strength programming, FFF has the capability to considerably meet this standard, e.g. a six component latex mixture, ranging from 20 to 426 nm in size, was fractionated with F4 within 10 min [76]. In terms of protein analytics, the size distribution of wheat proteins was investigated by separation of monomeric and polymeric specimen via F4/MALS [77]. An application in the same realm is represented in Fig. 7, where HSA is separated into individual components, including monomer, dimer, trimer and oligomers within 20 min. Subsequently, by minimizing the cross-flow rate to a short time, the resolution power of the systems is decreased and a soluble hmw aggregate fraction $>10^6$ Da can be detected. A similar experiment was described recently, when HSA was subjected to heat-stress in order to induce aggregation [78]. Aggregation-induced particulate matter was analysed by light obscuration, and a hmw aggregate fraction could be isolated with AF4, revealing molar masses of up to 10^8 Da. It may be noted, that the AF4/F4 analysis of protein aggregates obviously resembles analytical tasks in synthetic polymer chemistry. For instance, molar mass distributions of polyacrylamide flocculants in solution were investigated by separating the flocculants with F4 and further characterized with MALS [79,80].

Multi-protein analysis was performed by managing the AF4 separation of four proteins within 20 min. Thereby, the scope of molar masses covered the range from 29 kDa (carbonic anhydrase) up to 669 kDa (thyroglobulin) [81].

Generally, assessing the performance of a fractionating technique by the separation of samples containing two or more different proteins inheres one potential pitfall: as proteins tend to take a variegated shape—comprising fragmented and oligomeric as well as unfolded forms—there may arise difficulties in assigning one single peak to the appendant separated component, e.g. granulocyte colony stimulating factor (G-CSF) dimer (~39 kDa) may unify with the detection signal of erythropoeitin (38 kDa),

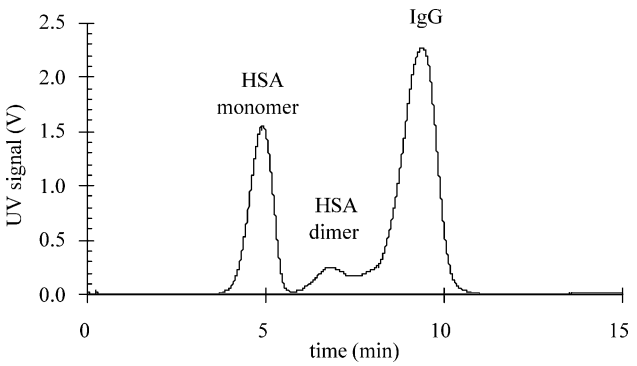

Fig. 8. AF4 separation of HSA solution containing γ-immunoglobulin. The overlap of UV_{280} signals of HSA dimer (133 kDa) and IgG (147 kDa) hampers data interpretation.

as both specimen reveal identical molar masses, thus exacerbating correct data interpretation. The matter is exemplified by the AF4 fractionation of albumin solution containing a γ-immunoglobulin (Fig. 8). Due to the ~10% molar mass difference between HSA dimer (133 kDa) and the immunoglobulin (147 kDa), a base-line separation is impeded, despite high-resolution conditions of 75% cross-flow.

Referring to the quantification of protein aggregation, SEC certainly represents the gold standard in both industry and science. Up to now, only two relevant comparative studies between FFF techniques and SEC have been performed. One study addressed the characterization of polystyrene standards in organic solvents by means of ThFFF and was mainly aimed at compiling the particular theoretical principles of each method [82]. In theory, FFF should offer a much higher resolution, since the MW-based selectivity is larger (0.5–0.7 versus 0.2 for SEC). Basically, this was substantiated by the second study, correlating the results of both AF4 and SEC in terms of antibody analytics [83]. Solutions of several immunoglobulins were stressed via rapid pH change and subsequently characterized. It was found that AF4 can provide higher selectivity and greater resolution which is maintained over a wider molecular weight range than in SEC. Unfortunately, antibody samples were prepared individually for AF4 and SEC analysis and different elution media for both techniques were chosen. Though, this study revealed the principal feasibility of AF4 in analysis of unprepared samples, allocating AF4 a greater application range and more informational power. In practice, AF4/F4 offers superior resolution for samples with MW $>$ 100 kDa, but lower resolution in the $<$50 kDa range [84].

Due to the lack of package material within the channel, AF4/F4 fractionations are performed under moderate conditions, avoiding shear stress. The system pressures normally exerted on the samples are below 5 bar. This predestines AF4 for characterization of hmw analytes, prone to artifacts due to experiment conditions, e.g. shear degradation and upper exclusion limit of the separation technique applied.

Referring to this, AF4 was employed to study conformational changes, aggregation tendencies and hmw ratios of macromolecules which are utilized in pharmaceutical industries, such as ethylhydroxyethyl cellulose, carrageenans and starch polysaccharides [85–87]. Furthermore, AF4 was employed to characterize amphiphilic polymers, where the usefulness of SEC is limited because of interactions between hydrophobic polymer segments and the stationary phase. Compared to SEC, adsorption phenomena in AF4 are minor, considering FFF channel surface areas of usually 30 cm^2 and SEC package material surface areas of $\geq$30,000 cm^2 [88]. However, the cross-flow induced analyte-membrane contact may somewhat annihilate this AF4 feature. In both techniques, the application of carrier liquids containing surfactants such as SDS or Tweens in order to reduce potential adsorption phenomena is popular [5,89].

Consequently, the aggregation of amphiphilic graft copolymers [90], essential for the stabilization of interfacial structures, was analyzed via AF4 as well as the aggregation of pullulan derivates [91].

Native conformational structure and intact folding are crucial parameters influencing protein drug efficacy, e.g. of antibodies and enzymes. The diffusion coefficient (D) is a fundamental physical parameter for the elucidation of macromolecular size and shape, providing information on surface corrugation and roughness of globular proteins. [92]. From D, the state of interaction between protein specimen or their degree of aggregation can be deduced. Considering that AF4 fractionation is due to differences in sample diffusion coefficients, AF4 can deliver valuable data on the structural uniformity of proteins and substantiate data obtained by other techniques, e.g. molar $absorbance_{400\ nm}$ or circular dichroism.[78]. As illustrated in Fig. 9,

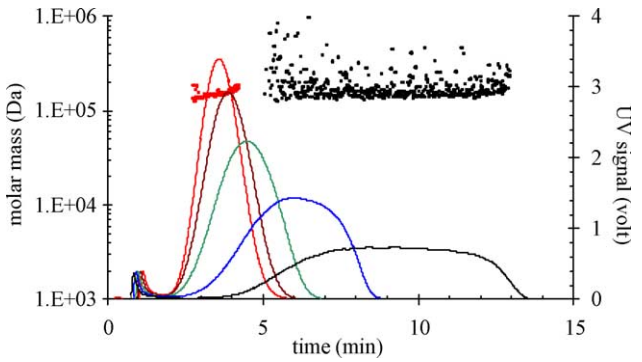

Fig. 9. Evaluation of 150 kDa immunoglobulin structural uniformity: the diffusion coefficient D is impacted by unfolding phenomena, e.g. due to denaturation. With increasing cross-flow exerted, present conformational alterations would mirror in peak corrugations. Note that the MW determined by MALS is not impacted by the cross-flow applied (150 kDa). The color of the solid UV_{280} signal lines and the MALS signals (dots) refer to separations with cross-flow intensities of 0% (red), 10% (brown), 20% (green), 30% (blue) and 40% (black) [78]. (For interpretation of the references to colour in this figure legend, the reader is referred to the web version of this article.)

the structural uniformity of a 150 kDa immunoglobulin can be scrutinized by subjecting the protein to successive AF4 runs, thereby applying various cross-flow intensities. Even at conditions with high system resolution—i.e. higher cross-flow applied—no bias peaks or peak shoulders can be detected, indicating structural uniformity.

In all applications described, the absence of package material within the FFF separation channel enables the characterization of insoluble analytes aside soluble specimens. Hence, AF4 may be predestined to the analysis of protein formulations of biopolymeric samples containing soluble, insoluble or precipitated protein specimen.

3.2. Colloids, cells and particulate matter—insoluble analytes

Due to its unique separation mode, one other main field of AF4 application represents the analysis of dissolved sample components aside undissolved particles. Moreover, the size limit of samples amenable to AF4 separation can be risen to the μm range, allowing the separation of nanoclusters, nanocolloids, microparticles and even cells.

These AF4 features were applied in the analysis of soluble poly(vinyl pyrrolidone) PVP and insoluble cross-linked poly[poly(vinylpyrrolidone)], which are prevalently used as pharmaceutical excipients [93]. AF4 was used to gain the first insights into the structure of molecular-composite PVP [94]. The two-phase nature of such systems was demonstrated, since AF4 yielded a soluble polymer fraction aside insoluble polymer particles. By means of on-line MALS detection, the particles were shown to reveal dimensions of ~350 nm in diameter.

Generally, colloids enjoy a widespread utilization as samples for AF4 analysis, as they represent ideal candidates to evaluate fractionation efficacy and resolution power. In this realm, mainly latex standards with dimensions between 25 and 800 nm are used. The combination of FFF techniques and MALS was shown in many cases to exceed the resolution power of other established analytical systems such as transmission electron microscopy [95].

The task of separating dissolved and undissolved sample components via AF4 was frequently performed in the course of biopharmaceutical applications, e.g. by examining the distribution of lipophilic drugs within human plasma or when characterizing lipoproteins originating from human blood [96]. An alternative frit-inlet AF4 technique was also successfully implemented in the separation of lipoprotein particles of coronary artery disease (CAD) patients [97]. The method described showed potential in implementing AF4 as a diagnosis tool in CAD, by characterizing the decrease of low density lipoprotein (LDL) particle sizes compared to those of LDL particles from healthy humans.

In particular, it was shown via F4 that the dimensional range as well as the concentrational distribution of human plasma lipoprotein fractions can vary between samples or individuals [57]. After analysing different human plasma samples using F4, the high density lipoprotein fraction was found to encompass a 4–16.5 nm size range, whereas the low density lipoprotein fraction was assessed to span 16.5–36 nm and the very low density lipoprotein fraction to span a 36–100 nm size range [98].

Pertaining to a broad-range analysis, F4 can be employed to accurately analyze colloidal and particulate systems running the gamut from nm to μm range, e.g. heterogeneous mixtures of cationic lipid-DNA colloidals were characterized via MALS in terms of shape and size distribution subsequent to separation by F4 [99].

A valuable feature of AF4 lies in the fact that individual components of complex mixtures can be characterized subsequent to isolation from the rest of the complex mixtures. Here, AF4 proves to be a powerful tool in the evaluation of analyte features not that readily accessible, if at all, with other techniques. In case of polyorganosiloxane nanocolloids, AF4 was used for analysis of nanoparticles dispersed in a complex mixture in the presence of excess surfactant [100]. Alternatively, the FFF potential for degradation-free separation was applied to provide analytes with extremely narrow size distributions for subsequent high-precision measurement of dimensions via MALS. In this respect, AF4/MALS showed to be superior to other established analytical methods [101].

Without doubt, the use of AF4 in biopharmaceutics will gain increasing momentum in the area of gene therapy. There, the design of ideal nanoparticulate carriers with the ability to target specific cell types is highly desired and the DNA delivery with non-viral vectors may be deemed one major challenge of the years ahead [102]. The ability of AF4 to fractionate gelatine nanoparticles was indicated only recently [78]. By means of MALS, the nanoparticles were assigned root mean square radii between 80 and 112 nm.

Pertaining to that, the huge AF4 application possibilities may be represented by the fractionation of nanoparticle–protein mixtures. Therefore, erythropoeitin was added to gelatin nanoparticle batches and the mixture was analyzed with AF4 (Fig. 10). Each of the presented modified elution profiles of the nanoparticle fractions can be realized by applying a decay of initial higher cross-flow rates (50%) down to 1% after an appropriate time. Similarly, the elution profile of the EPO fraction can be varied by exerting different cross-flow strengths in the initial stages of the separation experiments. The separation of nanoparticulate drug carriers from unbound oligonucleotide payload as well as the assessment of nanoparticulate drug carrier loading efficacy by means of AF4 was described recently [103]. In this respect, it can be referred to studies performed to characterize cationic lipid-DNA gene carrier complexes formed using different lipid-DNA ratios and to monitor changes in those complexes over time [104].

A further promising AF4 application lies in the field of vaccine control. The surface features of deactivated bacteria or viruses affect the immunoresponse to bacteria- or virus-associated antigens. Hence, sorting and characterization of

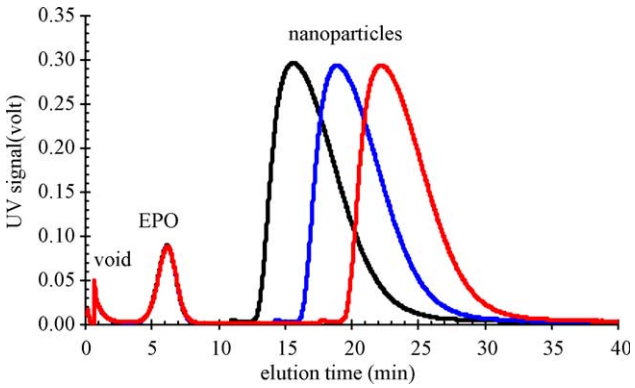

Fig. 10. Separations of erythropoeitin (~38 kDa) from nanoparticles applying a decay of initial constant 50% cross-flow to 1% after 13 min (black), 16.3 min (blue) and 19.7 min (red), respectively. The reproducibility of the separations is reflected by the overlap of $UV_{260\ nm}$ detector signals of both void peak and protein. (For interpretation of the references to colour in this figure legend, the reader is referred to the web version of this article.)

deactivated bacteria or viruses is an important way of quality control for whole-cell bacterial or viral vaccines and AF4 performance was successfully demonstrated [105]. In this context, also the separation of plasmids and plasmid fragments [74] as well as the determination of acid phosphatase in cultivation media via AF4 have to be subsumed [106].

Interestingly, the evaluation of the translation capacity of cells producing recombinant proteins can be realized by screening their ribosomal composition via AF4. Separation and determination of the level of tRNA, ribosome and ribosomal subunits via AF4 have already been reported [107–109]. Based on this, an optimized ribosome preparation method has been reported, including cell harvest, lysozyme treatment, detergent treatment as well as subsequent AF4 analysis and channel wash in less than 20 min [110]. This enables one to monitor change of several growth and production indicators in one individual experiment as well as high-frequency sampling. The separation of ribosomal material—i.e. the number of active 70S ribosomes and the overall number of 30S, 50S and 70S ribosomal particles and the tRNA level—are much faster than the alternative ultracentrifugation which can have analysis times of several hours [111].

Commensurate with the nowadays increased ecological awareness, AF4 is employed increasingly in analytics of environmental particles and macromolecules. This development is instanced by the characterization of humic substances and the separation of colloidal organic matter from river waters [112]. Similarly, the effects of ionic strength and electrolyte composition on the aggregation of fractionated humic substances were scrutinized [113]. By coupling AF4 with alternative detection systems, thermal lens spectroscopy was demonstrated to reveal improved sensitivity in the characterization of environmental hydrocolloids, especially for particle dimensions <20 nm [114]. As the molecular size of humic substances is still highly controversial, with reported molar masses in the range of 500–200,000 Da [115], the moderate and non-disruptive separation features of FFF appear tailor-made for studying sensitive substances.

3.3. Random walks

Considering that FFF was introduced to analytical science in the late 1960s and was long kept in a rather shadowy existence, by regarding the development in the last decade it is to be assumed that diversity and potential of FFF methods and especially AF4/F4 most probably will experience an upturn in the years ahead. Only recently, considerable effort was devoted to further investigating the underlying principles of AF4/F4 and bolster the theory with data based on experiments aimed at clarifying potential pitfalls of the method. For instance, the effects of the carrier ionic strength and carrier composition on the retention behavior of analytes in F4 were well enlightened [116]. The impact of sample concentration effects on retention was analyzed, indicating that retention deviations in case of compact particles are due to mean distance effects while in case of random coil behaving samples viscosity effects come into place [117]. In the characterization of particles by F4, corrections to standard retention theory that account for particle–wall interactions were investigated, based on theoretical calculations as well as on data derived by appropriate, target-oriented experiments [118]. Given that background, future analytical tasks can be approached by means of F4 even more efficaciously.

Due to the versatility of the technique, the use of AF4 is not restricted to the fractionation and characterization of drugs and excipients commonly used in pharmaceutics and biopharmaceutics, but can of course provide valuable data in many related fields, e.g. problems of sterility and particle contamination associated with the mass production of parenterals [119]. Referring to this, it is known that besides drug instability, particulate matter can emerge in parenterals/package materials during processing, e.g. by sterilization, freezing and lyophilization [120]. In order to scrutinize the sensitivity of AF4 in the fractionation of particulate matter, parenteral package containers were subjected to various processes that package materials normally encounter in the course of manufacturing and production of pharmaceuticals. To provoke particulate matter generation, 20R glass vials were sterilized by dry heat (180 °C, 20 min), filled with 5 ml Milli-Q™-water, stored at −80 °C for 24 h prior to further 24 h storage at 5 °C, were exposed to lyophilization applying state-of-the-art process parameters, and finally refilled by adding 5 ml Milli-Q™-water. Light obscuration data ascribed virtually no particulate contamination to sterilization and freeze/thaw processes, but the final lyophilization step accounted the lion's share of particulate contaminates. Conversely, AF4/MALS analysis of the sample batches prior/subsequent to the freeze/thaw cycle revealed a notable

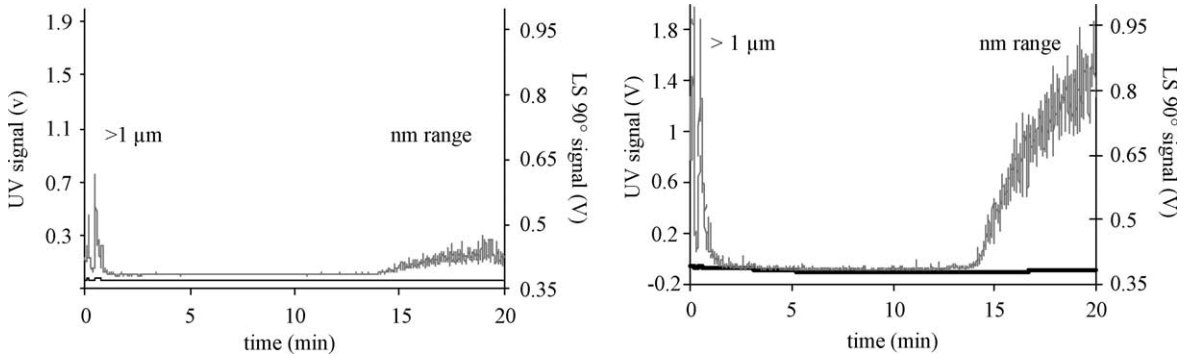

Fig. 11. Sensitivity of AF4/MALS in detection of particulate matter induced by manufacturing processes: parenteral package container volume prior (left) and subsequent (right) to freeze/thaw cycle (refer to text). Since the particles reveal no UV_{280} absorbance, UV spectrophotometry (black curve) fails detection—whereas the sensitivity of $MALS_{90°}$ (grey curve) is expressed by intense signals. AF4 parameters: 25% cross-flow is reduced to 0% after 13 min, forward flow 1 ml/min. Note that in this application light obscuration failed in detecting particle contamination.

increase of scattered light intensity due to particles in the higher nm range and µm range, which emerged during freeze/thawing (Fig. 11). Due to that, AF4 can present a valuable alternative in analytical challenges where particle counting techniques such as light obscuration detects no notable results, e.g. in the differentiation between protein solutions with and without visible particulate matter. AF4 recently succeeded in the fractionation of particulate samples in the two-digit µm range, thereby approaching sample components coming up to visibility [121].

Moreover, AF4 can be used in the field of disposable syringes for the parenteral application of drugs. The special features of those syringes are conferred by siliconization. Often, thin films of silicone oil are spread from diluted aqueous silicone oil emulsions on the inner barrel surface and successively heat treated above 300 °C for ~30 min. However, even after heat curing besides an immobilized bound component a soluble silicone oil fraction is present on the glass barrel surface. This soluble silicone oil is amenable to detachment, may permeate into the syringe volume and thereby result in (sub-)visible particulate matter via coalescence processes—thus potentially contravening regulatory standards. Notable increase in particle contamination of disposable siliconized syringes due to silicone oil detachment and potential interactions of drugs with silicone oil syringe coatings have repeatedly been reported [122–124]. Of crucial importance thereby is the question of the particulate matter origin—e.g. denatured and aggregated protein drug or silicone oil detachment and coalescence. Subjecting protein solution filled siliconized syringes which have already experienced silicone oil detachment to thermal stress renders three components amenable to AF4 separation—thereby simulating a worst-case scenario (Fig. 12): a fraction of silicone oil droplets, the native 147 kDa immunoglobulin drug, and a fraction of hmw protein aggregates. According to the principles of AF4 fractionation, the ~10 µm silicone oil droplets elute in steric mode conditions prior to the soluble protein. By means of on-line MALS coupling, the MW of both protein monomer and hmw aggregates can conveniently be assessed. This application demonstrates that AF4 can be a valuable tool for answering challenging questions, which otherwise could necessitate the application of an array of expensive analytical methods.

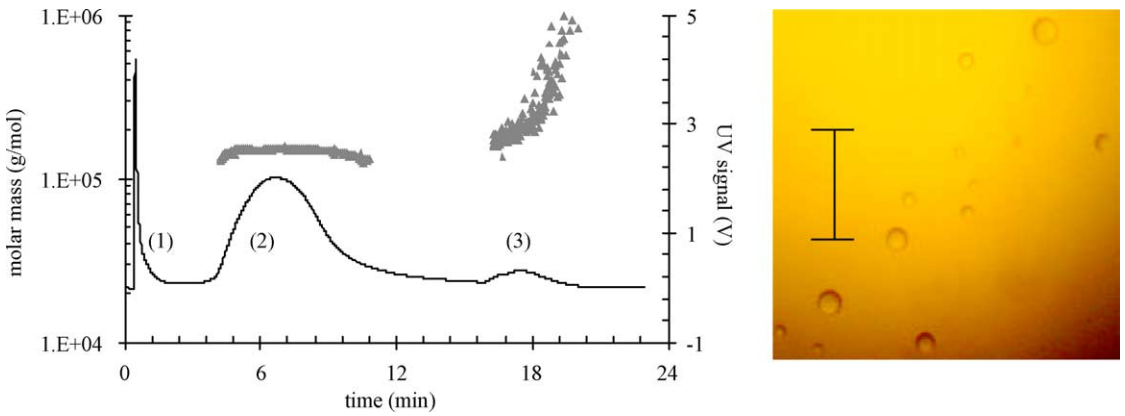

Fig. 12. Left: AF4 fractionation of a complex mixture of components in heat-stressed siliconized syringes: (1) silicone oil droplets, (2) protein drug monomer and (3) hmw protein aggregates. UV (black line) and $MALS_{90°}$ signal (grey line), the latter revealing a 150 kDa MW of the native monomers. Right: light microscopy analysis of the collected (1) fraction, scale bar representing 100 µm. Note the ideal spherical dimensions of the dispersed silicone oil droplets. (For interpretation of the references to colour in this figure legend, the reader is referred to the web version of this article.)

4. Conclusions

In this review the family of field-flow fractionation (FFF) was presented as a versatile and powerful analytical technique. The underlying principles as well as the system set-up of asymmetrical flow FFF (AF4) were introduced. Due to its unique features, AF4 may be deemed a valuable tool in biopharmaceutical analytics: soluble and insoluble sample specimen can be characterized concomitantly, and also complex mixtures of colloids, particles or even cells can be characterized. The possibility to subject non-prepared samples to AF4 analysis is a prerequisite for the quantification of hmw protein aggregates. Because the separation channel lacks a stationary phase/package material, even shear-sensitive samples can be analyzed. The resolution power can be universally modulated between two individual runs or even in one run, and sample fractions can be provided for subsequent on-line or off-line analysis. The wide application range, running the gamut from 1 nm up to ~ 100 μm, encompasses more applications than most other analytical techniques do. Moreover, the possibility to combine AF4 with highly sophisticated detection techniques like MALS or other methods like inductively coupled plasma (ICP) or electronspray mass spectroscopy may further fertilize the AF4 application range. Thereby, a convenient identification of the separated analytes by assessment of molar mass, hydrodynamic radius or chemical composition is possible.

Given the background of a tremendous demand for powerful and versatile analytical techniques in biopharmaceutical analytics today, and bearing in mind the valuable and unique features of AF4, a more widespread utilization of AF4 is to be expected.

References

[1] J.C. Giddings, A new separation concept bases on a coupling of concentration and flow nonuniformities, Sep. Sci. 1 (1966) 123–125.
[2] J.C. Giddings, Field-flow fractionation: analysis of macromolecular, colloidal, and particulate materials, Science 260 (1993) 1456–1465.
[3] S.S. Huang, Molecular weight separation of macromolecules by hydrodynamic chromatography, in: S. Wu (Ed.), Column Handbook for Size Exclusion Chromatography, Academic Press, New York, 1999, pp. 597–610.
[4] J. Bos, R. Tijssen, Hydrodynamic chromatography of polymers, J. Chromatogr. Libr. 56 (1995) 95–126.
[5] H. Coelfen, M. Antonietti, Field-flow fractionation techniques for polymer and colloid analysis, Adv. Polym. Sci. 150 (2000) 67–187.
[6] J.C. Giddings, Unified Separation Science, Wiley, New York, 1991.
[7] T. Pauck, H. Coelfen, Hydrodynamic analysis of macromolecular conformation. A comparative study of flow field-flow fractionation and analytical ultracentrifugation, Anal. Chem. 70 (1998) 3886–3891.
[8] J. Li, K.D. Caldwell, W. Maechtle, Particle characterization in centrifugal fields: comparison between ultracentrifugation and sedimentation field-flow fractionation, J. Chromatogr. 517 (1990) 361–376.
[9] M. Martin, P.S. Williams, Theoretical advancement in chromatography and related separation techniques, in: F. Dondi, G. Guiochon (Eds.), NATO ASI Series C, 383, Kluwer, Dordrecht, 1992, pp. 513–580.
[10] P.J. Wyatt, Light scattering and the absolute characterization of macromolecules, Anal. Chim. Acta 272 (1993) 1–40.
[11] P.J. Wyatt, Absolute measurements with FFF and light scattering, Polym. Mater. Sci. Eng. 65 (1991) 198–199.
[12] D. Roessner, W.M. Kulicke, On-line coupling of flow field-flow fractionation and multi-angle laser light scattering, J. Chromatogr. A 687 (1994) 249–258.
[13] G.E. Kassalainen, S.K. Williams, Coupling thermal field-flow fractionation with matrix-assisted laser desorption/ionization time-of-flight mass spectrometry for the analysis of synthetic polymers, Anal. Chem. 75 (2003) 1887–1894.
[14] H. Lee, S.K. Williams, Analysis of whole bacterial cells by flow field-flow fractionation and matrix assisted laser desorption/ionisation time-of-flight mass spectrometry, Anal. Chem. 75 (2003) 2746–2752.
[15] J. Janca, Field-flow fractionation, J. Chromatogr. Libr. 51A (1992) 449–479.
[16] H.C. Berg, E.M. Purcell, A method for separating according to mass a mixture of macromolecules or small particles suspended in a fluid, 3. Experiments in a centrifugal fluid, Proc. Natl Acad. Sci. USA 58 (1967) 1818–1821.
[17] F.J. Yang, M.N. Myers, J.C. Giddings, Programmed sedimentation field-flow fractionation, Anal. Chem. 46 (1974) 1924–1930.
[18] M.H. Moon, Sedimentation field-flow fractionation, in: M.E. Schimpf, K.D. Caldwell, J.C. Giddings (Eds.), Field-flow Fractionation Handbook, Wiley, New York, 2000, pp. 225–237.
[19] J.J. Kirkland, C.H. Dilks, W.W. Yau, Sedimentation field flow fractionation at high force fields, J. Chromatogr. 255 (1983) 255–271.
[20] J.J. Kirkland, W.W. Yau, W.A. Doerner, J.W. Grant, Sedimentation field flow fractionation of macromolecules and colloids, Anal. Chem. 52 (1980) 1944–1954.
[21] J.C. Giddings, B.N. Barman, M.K. Liu, Separation of cells by field-flow fractionation and related methods, in: D.S. Kompala, P. Todd (Eds.), Cell Separation Science and Technology, American Chemical Society, Washington, DC, 1991, pp. 128–144.
[22] X. Tong, K.D. Caldwell, Separation and characterization of red blood cells with different membrane deformability using steric field-flow fractionation, J. Chromatogr. B 674 (1995) 39–47.
[23] S.K. Williams, B. Butler-Veytia, H. Lee, Determining the particle size distributions of titanium dioxide using sedimentation field-flow fractionation and photon correlation spectroscopy, ACS Symp. Ser. 805 (2002) 285–298.
[24] B. Chen, R. Beckett, Development of SdFFF-ETAAS for characterising soil and sediment colloids, Analyst 126 (2001) 1588–1593.
[25] H.J. Tyrell, Diffusion and Heat Flows in Liquids, Butterworths, London, 1961.
[26] G.H. Thompson, M.N. Myers, J.C. Giddings, Observation of a field-flow fractionation effect with polystyrene samples, Sep. Sci. 2 (1967) 797–800.
[27] G.H. Thompson, M.N. Myers, J.C. Giddings, Thermal field-flow fractionation and polystyrene samples, Anal. Chem. 41 (1969) 1219–1222.
[28] J.C. Giddings, M. Marin, M.N. Myers, High-speed separations by thermal field-flow fractionation, J. Chromatogr. 158 (1978) 419–435.
[29] M.E. Schimpf, Thermal field-flow fractionation, in: M.E. Schimpf, K.D. Caldwell, J.C. Giddings (Eds.), Field-flow Fractionation Handbook, Wiley, New York, 2000, pp. 239–256.
[30] J. Janca, Micro-channel thermal field-flow fractionation: new challenge in analysis of macromolecules and particles, J. Liq. Chromatogr. Relat. Technol. 25 (2002) 683–704.

[31] J. Lou, Salt effect on separation of polyvinylpyridines by thermal field-flow fractionation, J. Liq. Chromatogr. Relat. Technol. 26 (2003) 165–175.
[32] M. Sibbald, L. Lewandowski, M. Mallamaci, E. Johnson, Multidisciplinary characterization of novel emulsion polymers, Macromol. Symp. 155 (2000) 213–228.
[33] A. van Asten, An exploration of thermal field-flow fractionation, Dissertation, Amsterdam, Holland, 1995.
[34] K.D. Caldwell, Y.-S. Gao, Electrical field-flow fractionation in particle separation, Anal. Chem. 65 (1993) 1764–1772.
[35] N. Tri, K.D. Caldwell, R. Beckett, Development of electrical field-flow fractionation, Anal. Chem. 72 (2000) 1823–1829.
[36] K.D. Caldwell, Electrical field-flow fractionation, in: M.E. Schimpf, K.D. Caldwell, J.C. Giddings (Eds.), Field-flow Fractionation Handbook, Wiley, New York, 2000, pp. 295–312.
[37] S.A. Palkar, M.R. Schure, Mechanistic study of electrical field flow fractionation. 1. Nature of the internal field, Anal. Chem. 69 (1997) 3223–3229.
[38] S.A. Palkar, M.R. Schure, Mechanistic study of electrical field flow fractionation. 2. Effect of sample conductivity on retention, Anal. Chem. 69 (1997) 3230–3238.
[39] J.C. Giddings, F.J. Yang, M.N. Myers, Flow field-flow fractionation: a versatile new separation method, Science 193 (1976) 1244–1245.
[40] P. Dycus, K.D. Healy, G.K. Stearman, M.J. Wells, Diffusion coefficients and molecular weight distributions of humic and fulvic acids determined by flow field-flow fractionation, Sep. Sci. Technol. 30 (1995) 1435–1453.
[41] S.K. Williams, Flow field-flow fractionation, in: M.E. Schimpf, K.D. Caldwell, J.C. Giddings (Eds.), Field-flow Fractionation Handbook, Wiley, New York, 2000, pp. 257–277.
[42] H.L. Lee, E.N. Lightfoot, Preliminary report on ultrafiltration-induced polarization chromatography—an analog of field-flow fractionation, Sep. Sci. 11 (1976) 417–440.
[43] J.C. Giddings, F.J. Yang, M.N. Myers, Flow field-flow fractionation as a methodology for protein separation and characterization, Anal. Biochem. 81 (1977) 395–407.
[44] J.C. Giddings, G.C. Lin, M.N. Myers, Fractionation and size analysis of colloidal silica by flow field-flow fractionation, J. Colloid Interface Sci. 65 (1978) 67–78.
[45] J.C. Giddings, G.C. Lin, M.N. Myers, Fractionation and size distribution of water soluble polymers by flow field-flow fractionation, J. Liq. Chromatogr. 1 (1978) 1–20.
[46] J. Granger, J. Dodds, D. Leclerc, N. Midoux, Flow and diffusion of particles in a channel with one porous wall: polarization chromatography, Chem. Eng. Sci. 41 (1986) 3119–3128.
[47] K.G. Wahlund, J.C. Giddings, Properties of an asymmetrical flow field-flow fractionation channel having one permeable wall, Anal. Chem. 59 (1987) 1332–1339.
[48] M.E. Schimpf, K.D. Caldwell, J.C. Giddings (Eds.), Field-flow Fractionation Handbook, Wiley, New York, 2000.
[49] K.G. Wahlund, Asymmetrical flow field-flow fractionation, in: M.E. Schimpf, K.D. Caldwell, J.C. Giddings (Eds.), Field-flow Fractionation Handbook, Wiley, New York, 2000, pp. 279–294.
[50] A. Litzén, K.G. Wahlund, Zone broadening and dilution in rectangular and trapezoidal asymmetrical flow field-flow fractionation channels, Anal. Chem. 63 (1991) 1001–1007.
[51] J.J. Kirkland, C.H. Dilks, Flow field-flow fractionation of polymers in organic solvents, Anal. Chem. 64 (1992) 2836–2840.
[52] M. Miller, PhD Thesis, Department of Chemistry, University of Utah, Salt Lake City, USA, 1996.
[53] K.D. Jensen, S.K. Williams, J.K. Giddings, High-speed particle separation and steric inversion in thin flow field-flow fractionation channels, J. Chromatogr. 746 (1996) 137–145.
[54] J.C. Giddings, P.S. Williams, M.A. Benincasa, Rapid break-through measurement of void volume for field-flow fractionation channels, J. Chromatogr. 627 (1992) 23–35.
[55] B. Wittgren, K.G. Wahlund, Effects of flow-rates and sample concentration on the molar mass characterisation of modified celluloses using asymmetrical flow field-flow fractionation-multi-angle light scattering, J. Chromatogr. A 791 (1997) 135–149.
[56] M.A. Benincasa, J.C. Giddings, Separation and molecular weight distribution of anionic and cationic water-soluble polymers by flow field-flow fractionation, Anal. Chem. 64 (1992) 790–798.
[57] P. Li, J.C. Giddings, Isolation and measurement of colloids in human plasma by membrane-selective flow field-flow fractionation: lipoproteins and pharmaceutical colloids, J. Pharm. Sci. 85 (1996) 895–898.
[58] K.D. Caldwell, Steric field-flow fractionation and the steric transition, in: M.E. Schimpf, K.D. Caldwell, J.C. Giddings (Eds.), Field-flow Fractionation Handbook, Wiley, New York, 2000, pp. 79–94.
[59] J.C. Giddings, Displacement and dispersion of particles of finite size in flow channels with lateral forces: field-flow fractionation and hydrodynamic chromatography, Sep. Sci. Technol. 13 (1978) 241–245.
[60] B.R. Min, S.J. Kim, K.-H. Ahn, M. Moon, Hyperlayer separation in hollow fiber flow field-flow fractionation: effect of membrane materials on the resolution and selectivity, J. Chromatogr. A 950 (2002) 175–182.
[61] K.D. Caldwell, T.T. Nguyen, M.N. Myers, J.C. Giddings, Observations on anomalous retention in steric field-flow fractionation, Sep. Sci. Technol. 14 (1979) 935–946.
[62] M.H. Moon, K.-M. Kim, Y. Byun, D. Pyo, Size characterization of core-shell poly(L-lactide) microspheres by flow/hyperlayer field-flow fractionation, J. Liq. Chromatrogr. Relat. Technol. 22 (1999) 2729–2740.
[63] J.G. Dos Ramos, C.A. Silebi, Submicron particle size and polymerization excess surfactant analysis by capillary hydrodynamic fractionation (CHDF), Polym. Int. 30 (1993) 445–450.
[64] E.F. Casassa, Y. Tagami, Equilibrium theory for exclusion chromatography of branched and linear polymer chains, Macromolecules 2 (1969) 14–26.
[65] J.C. Giddings, Hydrodynamic relaxation and sample concentration in field-flow fractionation using permeable wall elements, Anal. Chem. 62 (1990) 2306–2312.
[66] M.H. Moon, M.N. Myers, Experimental field-flow fractionation: practises and precautions, in: M.E. Schimpf, K.D. Caldwell, J.C. Giddings (Eds.), Field-flow Fractionation Handbook, Wiley, New York, 2000, pp. 225–237.
[67] M.H. Moon, P.S. Williams, D. Kang, I. Hwang, Field and flow programming in frit-inlet asymmetrical flow field-flow fractionation, J. Chromatogr. A 955 (2002) 263–272.
[68] P.S. Williams, M.C. Giddings, J.C. Giddings, A data analysis algorithm for programmed field-flow fractionation, Anal. Chem. 73 (2001) 4202–4211.
[69] P.S. Williams, J.C. Giddings, Theory of field-programmed field-flow fractionation with corrections for steric effects, Anal. Chem. 66 (1994) 4215–4228.
[70] G. Walsh, Pharmaceutical biotechnology products approved within the European Union, Eur. J. Pharm. Biopharm. 55 (2003) 3–10.
[71] S. Levin, Field-flow fractionation in biomedical analysis, Biomed. Chromatogr. 5 (1991) 133–137.
[72] K.D. Caldwell, Field-flow fractionation, Anal. Chem. 60 (1988) 959–971.
[73] A. Litzén, K.G. Wahlund, Application of an asymmetrical flow field-flow fractionation channel to the separation and characterization of proteins, plasmids, plasmid fragments, polysaccharides and unicellular algae, J. Chromatogr. 461 (1989) 73–87.
[74] C. Tank, Separation and characterization of complex polymers and colloids by means of field-flow fractionation, Dissertation, Technische Universität Berlin, Germany, 1995.
[75] A. Litzén, K.G. Wahlund, Effects of temperature, carrier composition and sample load in asymmetrical flow field-flow fractionation, J. Chromatogr. 548 (1991) 393–406.

[76] A.M. Botana, S.K. Ratanathanawongs, J.C. Giddings, Field-programmed flow field-flow fractionation, J. Microcolumn Sep. 7 (1995) 395–402.
[77] M. Southan, F. MacRitchie, Molecular weight distribution of wheat proteins, Cereal Chem. 76 (1999) 827–836.
[78] W. Fraunhofer, G. Winter, J. Zillies, C. Coester, Asymmetrical flow field-flow fractionation as new analytical tool in pharmaceutical biotechnology, New Drugs 2 (2003) 16–19.
[79] R. Hecker, A. Jefferson, P.D. Fawell, J.B. Farrow, The characterization of polyacrylamide flocculants by flow field-flow fractionation combined with multi-angle laser light scattering, Bi-annu. Int. Symp. Fundam. Miner. Proc., Quebec City, Canada (1999) 107–121.
[80] R. Hecker, P.D. Fawell, A. Jefferson, The agglomeration of high molecular mass polyacrylamide in aqueous solutions, J. Appl. Polym. Sci. 70 (1998) 2241–2250.
[81] M.H. Moon, I. Hwang, Hydrodynamic vs. focusing relaxation in asymmetrical flow field-flow fractionation, J. Liq. Chromatogr. Relat. Technol. 24 (2001) 3069–3083.
[82] J.J. Gunderson, J.C. Giddings, Comparison of polymer resolution in thermal field-flow fractionation and size-exclusion chromatography, Anal. Chim. Acta 189 (1986) 1–15.
[83] A. Litzén, J.K. Walter, H. Krischollek, K.G. Wahlund, Separation and quantitation of monoclonal antibody aggregates by asymmetrical flow field-flow fractionation and comparison to gel permeation chromatography, Anal. Biochem. 212 (1993) 469–480.
[84] Y. Jiang, M.E. Miller, P. Li, M.E. Hansen, Characterization of water-soluble polymers by flow FFF-MALS, Am. Lab. 32 (2000) 98–108.
[85] M. Andersson, B. Wittgren, K.G. Wahlund, Ultrahigh molar mass component detected in ethylhydroxyethyl cellulose by asymmetrical flow field-flow fractionation coupled to multiangle light scattering, Anal. Chem. 73 (2001) 4852–4861.
[86] P. Roger, B. Baud, P. Colonna, Characterization of starch polysaccharides by flow field-flow fractionation-multi-angle laser light scattering-differential refractometer index, J. Chromatogr. A 917 (2001) 179–185.
[87] B. Wittgren, J. Borgstroem, L. Piculell, K.G. Wahlund, Conformational change and aggregation of kappa-carrageenan studied by flow field-flow fractionation and multiangle light scattering, Biopolymers 45 (1998) 85–96.
[88] T. Klein, C. Huerzeler, Characterization of biopolymers, proteins, particles and colloids by means of field-flow fractionation, GIT Laborfachzeitschrift 11 (1999) 1224–1228.
[89] H.G. Barth, B.E. Boyes, C. Jackson, Size exclusion chromatography, Anal. Chem. 66 (1994) 595–620.
[90] B. Wittgren, K.G. Wahlund, H. Dérand, B. Wesslén, Aggregation behaviour of an amphiphilic graft copolymer in aqueous medium studied by asymmetrical flow field-flow fractionation, Macromolecules 29 (1996) 268–276.
[91] C. Duval, D. le Cerf, L. Picton, G. Muller, Aggregation of amphiphilic pullulan derivatives evidenced by on-line flow field-flow fractionation/multiangle laser light scattering, J. Chromatogr. B 753 (2001) 115–122.
[92] J. Choi, M. Terazima, Denaturation of a protein monitored by diffusion coefficients: myoglobin, J. Phys. Chem. B 106 (2002) 6587–6593.
[93] E. Barabas, in: H.F. Mark (Ed.), Encyclopedia of Polymer Science and Engineering, vol. 17, Wiley, New York, 1989, p. 198.
[94] D.K. Hood, L. Senak, S.L. Kopolow, M.A. Tallon, Y.T. Kwak, D. Patel, J. MacKittrick, Structural insights into a novel molecular-scale composite of soluble poly(vinyl pyrrolidone) supporting uniformly dispersed nanoscale poly(vinyl pyrrolidone) particles, J. Appl. Polym. Sci. 89 (2003) 734–741.
[95] P.J. Wyatt, Submicrometer particle sizing by multiangle light scattering following fractionation, J. Colloid Interface Sci. 197 (1998) 9–20.
[96] M. Madorin, P. van Hoogevest, R. Hilfiker, B. Langvost, G.M. Kresbach, M. Ehrat, H. Leuenberger, Analysis of drug/plasma protein interactions by means of asymmetrical flow field-flow fractionation, Pharm. Res. 14 (1997) 1706–1712.
[97] I. Park, K.-J. Paeng, Y. Yoon, J.-H. Song, M.H. Moon, Separation and selective detection of lipoprotein particles of patients with coronary artery disease by frit-inlet asymmetrical flow field-flow fractionation, J. Chromatogr. B 780 (2002) 415–422.
[98] P. Li, M. Hansen, Protein complexes and lipoproteins, in: M.E. Schimpf, K.D. Caldwell, J.C. Giddings (Eds.), Field-flow Fractionation Handbook, Wiley, New York, 2000, pp. 433–470.
[99] H. Lee, S.K. Williams, S.D. Allison, T.J. Anchordoquy, Analysis of self-assembled cationic lipid-DNA gene carrier complexes using flow field-flow fractionation and light scattering, Anal. Chem. 73 (2001) 837–843.
[100] N. Jungmann, M. Schmidt, M. Maskos, Characterization of polyorganosiloxane nanoparticles in aqueous dispersion by asymmetrical flow field-flow fractionation, Macromolecules 34 (2001) 8347–8353.
[101] P.J. Wyatt, D.N. Villalpando, High-precision measurement of submicrometer particle size distributions, Langmuir 13 (1997) 3913–3914.
[102] G. Kaul, M. Amiji, Long-circulating poly(ethylene glycol)-modified gelatin nanoparticles for intracellular delivery, Pharm. Res. 19 (2002) 1061–1067.
[103] W. Fraunhofer, G. Winter, C. Coester, Asymmetrical flow field-flow fractionation and multi-angle light scattering for analysis of gelatin nanoparticle drug carrier systems, Anal. Chem. 76 (2004) 1909–1924.
[104] R. Williams, H. Lee, G. Kassalainen, Recent Advances in Field-flow Fractionation: Separations of Proteins, Gene-delivery Complexes, and Bacteria, ACS National Meeting, Book of Abstracts, San Francisco, CA, 2000.
[105] P. Reschiglian, A. Zattoni, B. Roda, S. Casolari, Bacteria sorting by field-flow fractionation. Application to whole-cell *Escherichia coli* vaccine strains, Anal. Chem. 74 (2002) 4895–4904.
[106] A. Litzén, M.B. Garn, H.M. Widmer, Determination of acid phosphatase in cultivation medium using asymmetrical flow field-flow fractionation, J. Biotechnol. 37 (1994) 291–295.
[107] M. Nilsson, S. Birnbaum, K.G. Wahlund, Determination of relative amounts of ribosome and subunits in *Escherichia coli* using asymmetrical flow field-flow fractionation, J. Biochem. Biophys. Methods 33 (1996) 9–23.
[108] M. Nilsson, L. Bulow, K.G. Wahlund, Use of flow field-flow fractionation for the rapid quantitation of ribosome and robosomal subunits in *Escherichia coli* at different protein production conditions, Biotechnol. Bioeng. 54 (1997) 461–467.
[109] V. Roos, C.I.J. Andersson, C. Arvfidsson, K.G. Wahlund, Expression of double Vitreoscilla hemoglobin enhances growth and alters ribosome and tRNA levels in *Escherichia coli*, Biotechnol. Prog. 18 (2002) 652–656.
[110] C. Arfvidsson, K.G. Wahlund, Time-minimized determination of ribosome and tRNA levels in bacterial cells using flow field-flow fractionation, Anal. Biochem. 313 (2003) 76–85.
[111] S. Birnbaum, J.E. Bailey, Plasmid presence changes the relative levels of many host cell proteins and ribosome components in recombinant *Escherichia coli*, Biotechnol. Bioeng. 37 (1991) 736–745.
[112] M. Benedetti, J.F. Ranville, M. Ponthieu, J.P. Pinheiro, Field-flow fractionation characterization and binding properties of particulate and colloidal organic matter from the Rio Amazon and the Rio Negro, Org. Geochem. 33 (2002) 269–279.
[113] M.A. Benincasa, G. Cartoni, N. Imperia, Effects of ionic strength and electrolyte composition on the aggregation of fractionated humic substances studied by flow field-flow fractionation, J. Sep. Sci. 25 (2002) 405–415.
[114] A. Exner, U. Panne, R. Niessner, Characterization of environmental hydrocolloids by asymmetric flow field-flow fractionation and thermal lens spectroscopy, Anal. Sci. 17 (2001) 571–573.

[115] J.S. Gaffney, N.A. Marley, S.B. Clark (Eds.), Humic and Fulvic Acids. Isolation, Structure and Environmental Role, ACS Symposium Series 651, Washington, DC, 1996, pp. 2–16.
[116] M.-A. Benincasa, K.D. Caldwell, Flow field-flow fractionation of poly(ethylene oxide) effect of carrier ionic strength and composition, J. Chromatogr. A. 925 (2001) 159–169.
[117] M. Martin, F. Feuillebois, Onset of sample concentration effects on retention in field-flow fractionation, J. Sep. Sci. 26 (2003) 471–479.
[118] Q. Du, M.E. Schimpf, Correction for particle-wall interactions in the separation of colloids by flow field-flow fractionation, Anal. Chem. 74 (2002) 2478–2485.
[119] J.Z. Knapp, Absolute sterility and absolute freedom from particle contamination, PDA J. Pharm. Sci. Technol. 52 (1998) 173–181.
[120] J. Gebhardt, N.A. Grumbridge, A. Knoch, Particulate contamination from siliconized rubber closures for freeze-drying, PDA J. Pharm. Sci. Technol. 50 (1996) 24–29.
[121] K.G. Wahlund, A. Zattoni, Size separation of supermicrometer particles in asymmetrical flow field-flow fractionation. Flow conditions for rapid elution, Anal. Chem. 74 (2002) 5621–5628.
[122] T. Sendo, K. Otsubo, A. Hisazumi, T. Aoyama, R. Oishi, Particle contamination in contrast media induced by disposable syringes, J. Pharm. Sci. 84 (1995) 1490–1491.
[123] B. Kobo, Intravenous (I.V.) fluid administration systems and incompatibility of injections, Yakugaku Zasshi 110 (1990) 1–15.
[124] R.K. Bernstein, Clouding and deactivation of clear (regular) human insulin: association with silicone oil from disposable syringes?, Diabetes Care 10 (1987) 786–787.